American Mineralogist, Volume 79, pages 737–744, 1994

Cooling rate histories from garnet + biotite equilibrium

KARIN EHLERS,* ROGER POWELL
School of Earth Sciences, University of Melbourne, Parkville, Victoria 3052, Australia
KURT STÜWE
Department of Geology and Geophysics, University of Adelaide, Adelaide, South Australia 5005, Australia

ABSTRACT

Dodson's (1986) solution of the temperature-dependent diffusion equation may be used to determine cooling histories from geothermometrically inferred closure temperatures. If a mineral pair such as garnet + biotite equilibrated at the start of cooling and continued to equilibrate during cooling, then such closure temperatures, T_c, are a strong function of grain size and cooling rate (s). Thus garnet grains of different sizes that equilibrated with biotite within one rock or thin section will close at different temperatures and thus should record different stages of the thermal history. The application of Dodson's equation in the deduction of thermal histories is straightforward if the position of the cut through a garnet grain is known. Unfortunately, the position of the section is normally unknown. However, with the use of a single garnet grain cut at an unknown position, an apparent closure temperature can be determined from an exchange geothermometer, and an apparent cooling rate can be calculated from the observed radius. From this apparent closure temperature and apparent cooling rate, a family of solutions of possible actual closure temperatures and cooling rates can be calculated for a family of assumed actual grain radii. This family of solutions forms a locus on a ln s vs. T_c diagram. With many analyses of garnet grain centers in one thin section, garnets of a particular size that give higher closure temperatures normally are cut closer to their centers. Using this practice, the cooling history of a rock may be determined. This approach was tested with a Monte Carlo simulation. The calculated cooling histories provide potentially important constraints on the tectonic evolution of metamorphic terrains.

INTRODUCTION

The pressure-temperature-time history of metamorphic rocks is the key to understanding the tectonic evolution of high-grade metamorphic terrains. One critical parameter of this history is the cooling path followed subsequent to the metamorphic temperature peak. Several studies have emphasized the characteristic shapes of cooling paths in different tectonic settings (e.g., Thompson and England, 1984; Lux et al., 1986; Sandiford et al., 1991). Importantly, it has been shown that cooling paths resulting from erosion-driven exhumation (England and Thompson, 1984) have a qualitatively different shape from those for advectively heated terrains (Sandiford et al., 1991). Cooling rates may be obtained from a series of ages using isotopic systems that have different closure temperatures. Alternatively, they may be inferred, in principle, from temperature-dependent element distributions in ion-exchange systems (Lasaga, 1983; Lasaga et al., 1977; Onorato et al., 1979; Ozawa, 1984; Jenkin et al., 1991). In petrologic systems, the temperature given by exchange geothermometry using the compositions of two coexisting minerals is known as the closure temperature. If the two minerals have reequilibrated during cooling, the closure temperature will be lower, possibly much lower, than the metamorphic peak temperature (Fig. 1).

Dodson (1973) was the first to derive an analytical solution for closure temperature as a function of cooling rate, grain size, and diffusional parameters. Evaluation of closure temperature from geothermometry allows an estimate of the cooling rate at the closure temperature. Moreover, as closure of the centers of larger grains takes place at a higher temperature than closure of the centers of smaller grains, it may be possible to determine the cooling rate histories from the closure relationships of different sized grains. This paper evaluates the possibility of determining cooling rate histories from measured closure temperatures using Fe-Mg exchange between garnet and biotite combined with the closure temperature development of Dodson (1986).

DODSON'S EQUATION

Dodson (1973, 1986) derived an analytical solution for the diffusion equation with a temperature-dependent diffusion coefficient for the following assumptions: (1) At the start of cooling, the minerals are in equilibrium, i.e.,

* Present address: Victorian Institute of Earth and Planetary Sciences, Department of Earth Sciences, Monash University, Clayton, Victoria 3168, Australia.

0003–004X/94/0708–0737$02.00

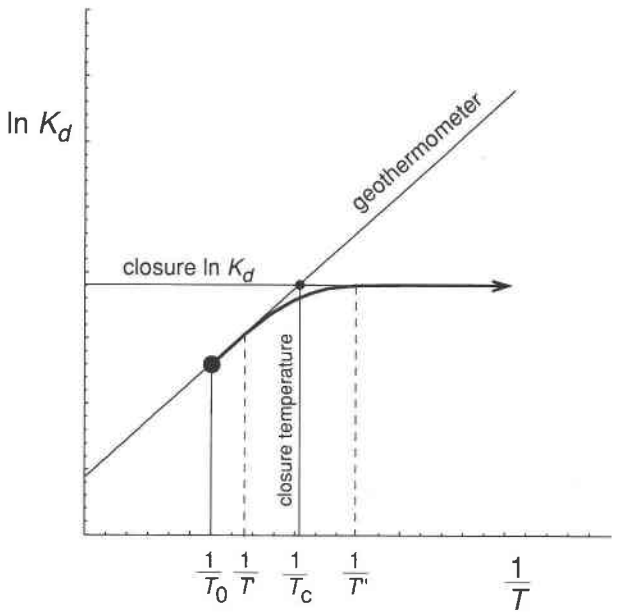

Fig. 1. The ln K_D vs. $1/T$ diagram illustrating the meaning of closure temperature (see also Spear and Peacock, 1989). The line defined by the geothermometer equation is indicated. At the peak temperature, T_0, a mineral pair at equilibrium sits on the geothermometer line. As temperature decreases during cooling, the mineral pair moves down the geothermometer line as diffusion ensures the maintenance of equilibrium. Eventually, as diffusion slows with the decrease of temperature, at some temperature, T', departure from the line starts. Then at some lower temperature, T'', the minerals cease to change composition and ln K_D no longer changes. The closure temperature, T_c, is the temperature given by the intersection of a line at the final ln K_D with the geothermometer line. Although this temperature does not correspond to any event in the cooling history of the mineral pair, it does lie between T' and T''.

Table 1. Notation

D_0	preexponential diffusion coefficient of the slower diffusing phase
D_{fast}	diffusion coefficient of the faster diffusing phase
D_{slow}	diffusion coefficient of the slower diffusing phase
$G(x)$	closure as a function of position in the grain, x
$G(y)$	closure as a function of section position, y
K_D	equilibrium constant
l	actual grain radius
l'	apparent grain radius
l_{fast}	actual grain radius of the faster diffusing phase
l_{slow}	actual grain radius of the slower diffusing phase
Q	activation energy of the slower diffusing phase
R	gas constant
s	cooling rate
$s(y)$	cooling rate calculated as a function of y
t	time
t_0	time at T_0
T_0	initial temperature
$T_c(x)$	closure temperature as a function of position in a grain x
$T_c'(y)$	closure temperature as a function of section position y
X^g_{Mg}	mole fraction of Mg in garnet [Mg/(Mg + Fe)]^g
X^{bi}_{Mg}	mole fraction of Mg in biotite [Mg/(Mg + Fe)]^{bi}
x	position in a grain (0 = center, 1 = edge)
y	section position in a grain (0 = center, 1 = edge)

the initial concentrations of the minerals are homogeneous. (2) The modal abundance of the faster diffusing mineral is very large, such that the concentration of the faster diffusing mineral does not change composition during reequilibration during cooling. (3) Diffusion is independent of concentration and the concentration of the diffusing species is small. (4) The closure temperature is sufficiently lower than the initial temperature, so that the closure temperature does not depend on these initial conditions. (5) Diffusion in one mineral is much faster than in the other, such that the closure temperature depends only on the diffusion properties of the slower diffusing phase. (6) Cooling histories change uniformly in reciprocal temperature with the time during closure.

Dodson's equation gives the closure temperature, $T_c(x)$, as a function of the position, x, in the slower diffusing phase (with $x = 0$ referring to the center of the grain and $x = 1$ the rim):

$$\frac{Q}{RT_c(x)} = \ln\left[\frac{D_0}{l^2}\cdot\frac{RT_c(x)^2}{Qs}\right] + G(x). \quad (1)$$

The notation is outlined in Table 1. Ehlers and Powell (1994) examined the applicability of Dodson's equation to cation exchange during cooling in the one-dimensional case involving a faster and a slower diffusing grain in which the interdiffusion coefficient is not a function of composition. They showed that Equation 1 (1) applies to interdiffusion between minerals of finite grain size; (2) applies when the concentrations of diffusing components are not small; if this effect in combination with the last is large, then an additional term is needed to account for the deviation from Dodson's equation; (3) gives closure temperatures that are independent of initial temperature, T_0, if $T_c/T_0 < 0.95$, and that are solely dependent on the slower diffusing phase if $D_{fast}/D_{slow} > 50$; (4) is applicable to a range of cooling histories, not just those that are linear in reciprocal temperature (see also Lovera et al., 1989).

In applying Dodson's equation to garnet + biotite equilibrium, and with respect to the above, Equation 1 was used here in its spherical form [affecting only $G(x)$], so that the garnet grains were considered to be spheres and surrounded by biotite. In addition, the combined grain size and concentration constraints of Ehlers and Powell were assumed to apply in the three-D case, with grain size becoming a volume constraint (unpublished work). The modal proportion of biotite should be at least 1.5 times that of the garnet if the garnet is completely surrounded by biotite (as it is taken to be in the simulations below). If the garnet is not completely surrounded by biotite, the situation is more complicated (see below).

The form of the dependence of closure temperature, $T_c(x)$, on the position in the slower diffusing phase, x, as given by Equation 1 is illustrated in Figure 2. The curve displays the closure temperature dependence on position of a grain cut through its center. However, in thin section the position of the grain section with respect to its center is unknown. Observation yields an apparent grain radius,

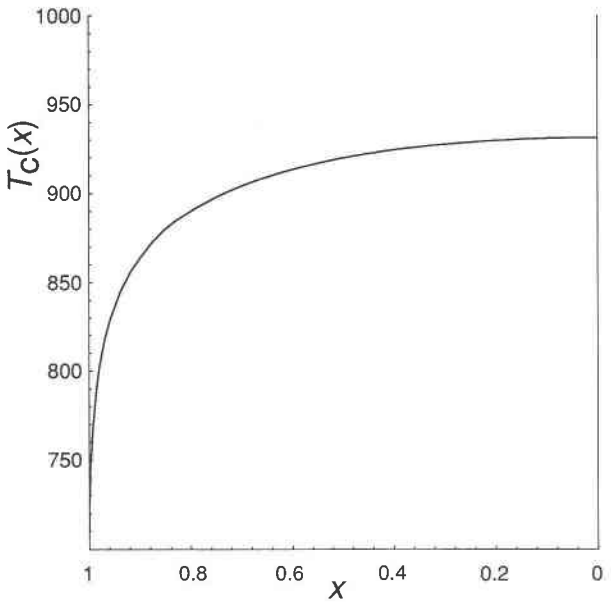

Fig. 2. The calculated closure temperature $T_c(x)$ as a function of position in the slower diffusing phase for a grain of radius $l = 0.05$ cm cut through its center (all diagrams calculated for $s = 10$ K/m.y., $D_0 = 9.81 \times 10^{-9}$ m²/s and $Q = 239$ kJ/mol). This curve is the closure temperature equivalent of the closure profile of Dodson (1986).

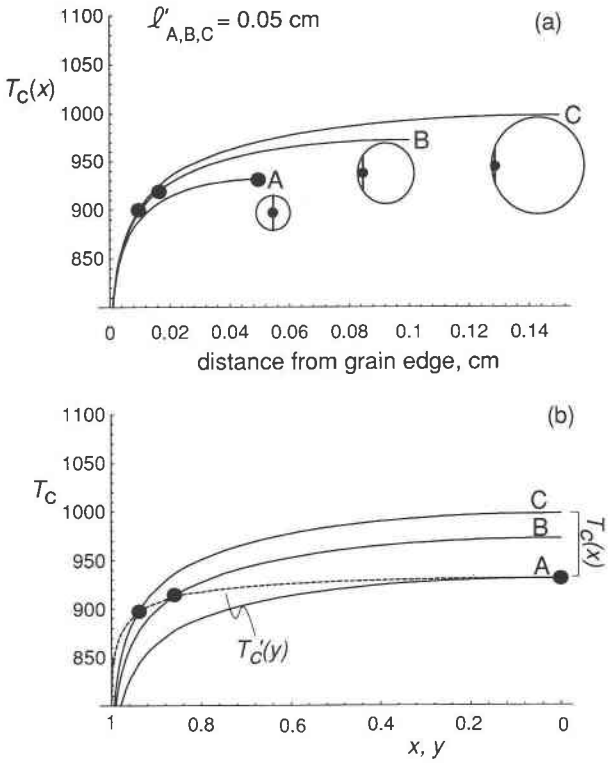

Fig. 3. (a) The closure temperature profiles of three garnet grains (A, B, C), with actual radii of 0.05, 0.10, and 0.15 cm, respectively. The closure temperatures for grains cut to have a radius of 0.05 cm are marked with solid circles. Note that the apparent closure temperatures decrease from A to C: grains cut closer to their centers having a particular apparent size give higher closure temperatures. (b) The same closure temperatures, $T_c(x)$, in terms of x (solid lines), with the locus of the closure temperatures, $T_c'(y)$, for the particular apparent grain radius of 0.05 cm shown in terms of y (dashed line). Along the dashed line, the actual grain radius varies according to $l = 0.05/\sqrt{1 - y^2}$. See Fig. 2.

l', at an unknown distance from the grain center, y ($y = 0$ refers to a grain cut through its center, $y = 1$ to a cut through the edge). One apparent grain radius, l', may correspond to any actual grain radius, l, larger than l', depending on y, from the equation of a circle $l = l'/\sqrt{1 - y^2}$.

Closure temperatures calculated from the centers of grains of unknown y are denoted $T_c'(y)$. With observed l' and the assumption that $y = 0$ so that $l = l'$, Equation 1 can be written

$$\frac{Q}{RT_c'(0)} = \ln\left[\frac{D_0}{l'^2}\cdot\frac{RT_c'(0)^2}{Qs}\right] + G(0). \quad (2)$$

For arbitrary y, so that $l = l'/\sqrt{1 - y^2}$, Equation 1 can be written

$$\frac{Q}{RT_c'(y)} = \ln\left[\frac{D_0}{l'^2}(1 - y^2)\frac{RT_c'(y)^2}{Qs}\right] + G(y). \quad (3)$$

The relationship between $T_c(x)$, as given by Equation 1, and $T_c'(y)$, as given by Equation 3, is illustrated in Figure 3 for three grains of different grain size that have reequilibrated during cooling at $s = 10$ K/m.y. Figure 3a shows the dependence of the closure temperature $T_c(x)$ on position in the grain for the three grains. In Figure 3b, the solid curves and circles correspond to those in Figure 3a but are plotted against x. The dashed curve, connecting the solid circles, gives $T_c'(y)$ as a function of y for the one apparent grain size of $l' = 0.05$ cm. This shows that grains of a particular radius give higher closure temperatures if they are cut nearer their centers. This feature is used to determine the cooling path for rocks.

Estimating cooling rates

In contrast to many of the isotopic applications for which Dodson derived Equation 1, in the case of cation exchange, an independent estimate of the closure temperature is available. This is always true when the diffusion is driven by the temperature dependence of an equilibrium at the interface between the slower diffusing phase and the faster diffusing phase surrounding it. When Fe-Mg exchange between slower diffusing garnet and faster diffusing biotite is considered, the closure temperature is estimated with the garnet-biotite thermometer. The closure relationships are reflected in the Fe-Mg zoning of the garnet produced as it attempts to equilibrate with the surrounding biotite during cooling. In relation to Figure 2, such a closure profile would be obtained by applying the thermometer to the composition of the garnet at each

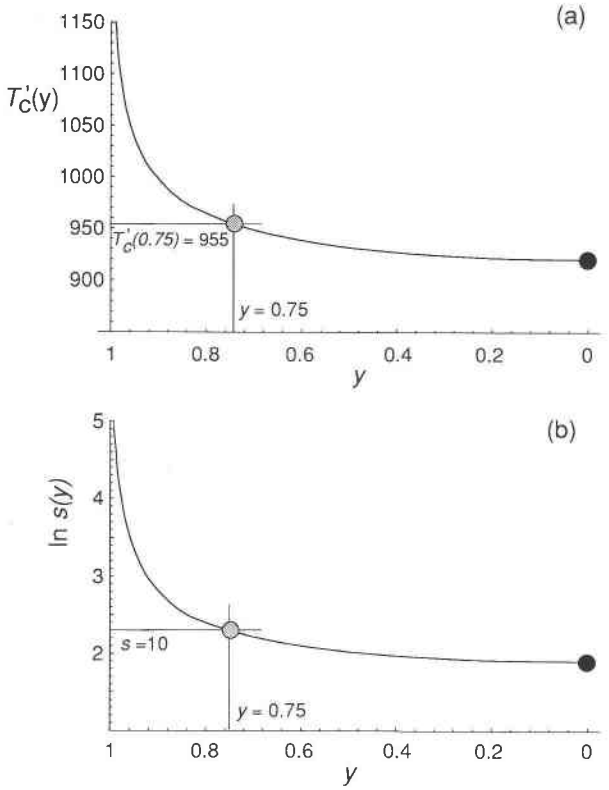

Fig. 4. Closure temperature and cooling rate relationships corresponding to an independent estimate of 920 K for the closure temperature at the center of an observed slower diffusing grain of radius $l' = 0.05$ cm (parameters as in Fig. 2, with $l = 0.0756$ cm and $y = 0.75$). The closure temperature (**a**) and cooling rate (**b**) are shown as functions of y. Solid circles mark the closure temperatures from the observed grain centers. Gray circles correspond to the closure temperature of the actual grain center.

position in the zoning profile with the biotite surrounding the garnet.

With an independent estimate of closure temperature from the Fe-Mg garnet-biotite thermometer, Dodson's equation can be used directly to estimate cooling rates if the cooling rate does not change during closure and if the position in the grain, x, is known. Then rearranging Equation 1 gives

$$s = \frac{D_0}{l^2}\cdot\frac{RT_c(x)^2}{Q}\exp\left[-\frac{Q}{RT_c(x)} + G(x)\right]. \quad (4)$$

Note that because closure temperature, $T_c(x)$, occurs in the exponential term, a small error in $T_c(x)$, and therefore in x, leads to a large error in s (for example, an error in T_c of 50 °C yields an error of approximately 1 log unit in s). It is important to realize that the cooling rate calculated from Equation 4 is the cooling rate at the closure temperature. Therefore, in principle, the variation of cooling rate over a range of closure temperatures can be calculated. The primary control is grain size: the centers of large garnet grains close at higher temperatures than the centers of smaller grains. Consequently, changes of the cooling rate with temperature may be recorded in the minerals for a significant part of the cooling history.

Given that x (or alternatively y) is generally not known, Equation 4 is not a practical equation in cooling rate estimation. However, Equation 3 produces

$$s(y) = \frac{D_0}{l'^2}(1 - y^2)\frac{RT_c'(y)^2}{Q}\exp\left[-\frac{Q}{RT_c'(y)} + G(y)\right] \quad (5)$$

where cooling rate is dependent on the position of section, $s(y)$. For a grain cut through its center, $y = 0$, the geothermometric T is $T_c'(0)$, and Equation 5 gives $s(0)$ directly. However, if y assumes an arbitrary value, then the geothermometric T must be adjusted to find the value corresponding to the actual center of the grain. This adjustment depends on the cooling rate, so the resulting application of Equation 5 is iterative. For example, consider a garnet grain with radius $l = 0.0756$ that cooled at $s = 10$ K/m.y., whose actual center gives a closure temperature of 955 K (Fig. 4). The garnet is cut at $y = 0.75$, giving an apparent radius of $l' = 0.05$ cm. A geologist observing this garnet measures $l' = 0.05$ cm and from the center of the observed grain calculates a closure temperature of 920 K from the geothermometer and a cooling rate of 6.7 K/m.y. from Equation 5. The calculation of the cooling rate is done by assuming that the observed grain is cut through its center, so that $y = 0$ and this cooling rate is $s(0)$. Analogously, the closure temperature is $T_c'(0)$. These assumptions give the solid circles in Figure 4a and 4b. However, if the garnet is not cut through its center, $y > 0$ and the corresponding $T_c'(y)$ and $s(y)$ are larger than $T_c'(0)$ and $s(0)$, respectively. With increasing y from 0, l increases by $l = l'/\sqrt{1 - y^2}$, such that $T_c'(y)$ and $s(y)$ can be calculated iteratively by means of Equation 5, giving the curves in Figure 4. Such curves may be represented as a locus along which y varies (Fig. 5). The curves must pass through the conditions used to set up the illustration (gray circles in Figs. 4, 5). It is important to note that the apparent closure temperature $T_c'(0)$, and cooling rate, $s(0)$, always define the low temperature and low cooling rate end of the locus. Consequently, the actual closure temperature and cooling rate can only be higher than the apparent values because in the limiting case the apparent grain center corresponds to the actual center.

In examining a locus (e.g., Fig. 5), there is no a priori method of identifying the actual closure temperature and cooling rate, which may lie anywhere on its locus. However, if many garnet-biotite pairs are analyzed from one rock or outcrop, it is usually possible to identify garnets that are most likely to be cut near their centers by comparing closure temperatures with similar observed grain radii (Fig. 3a). A range of closure temperature at a particular grain size can be seen on a $T_c'(0)$ vs. l' plot (Fig. 6a). From the form of Equation 3, grains cut near their centers should lie on a line of unit slope when $Q/RT_c'(0)$ is plotted against $2 \ln 1/l'$, and grains cut away from their centers should plot below this line, at lower temperatures. The best grains are those with values lying above a re-

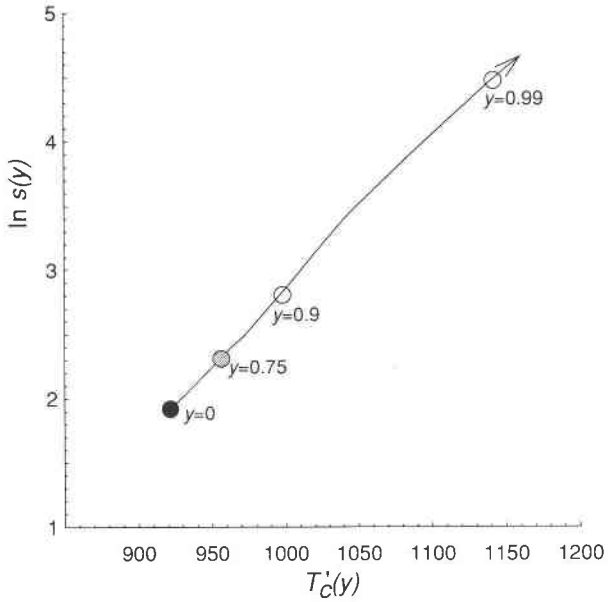

Fig. 5. The locus of $T'_c(y)$ vs. ln $s(y)$ for the example portrayed in Fig. 4. The solid and gray circles are as in Fig. 4.

gression line of unit slope (solid circles in Fig. 6b). The proviso is that this only works if the cooling rate does not change rapidly during cooling. For rapidly changing cooling rates, for example E in Figure 7, all grains may be used to identify such cooling histories (see below).

Application to garnet + biotite equilibria

The closure of Fe-Mg exchange between garnet and biotite is used as an example in the evaluation of determining cooling rates from geothermometric information. The closure temperature, $T_c(x)$, can be calculated using the garnet-biotite geothermometer equation formulated for iron-magnesium garnet and biotite. The data of Holland and Powell (1990) and the assumption of ideal mixing of Fe and Mg in garnet and biotite give

$$T_c(x) = \frac{44.97}{0.01456 + 3R \ln K_D(x)} \quad (6)$$

with the equilibrium constant, $K_D(x)$, given by

$$K_D(x) = \frac{[1 - X^{g}_{Mg}(x)]}{X^{g}_{Mg}(x)} \frac{X^{bi}_{Mg}}{(1 - X^{bi}_{Mg})}.$$

X^{g}_{Mg} and X^{bi}_{Mg} are the mole fraction of Mg in garnet and biotite, respectively. The mole fraction of Mg in garnet is a function of x (or y). However, to fulfill the requirement of Equation 1, the mole fraction of Mg in biotite should not be a function of x.

In Equation 4, we follow Cygan and Lasaga (1985) in using the Mg self-diffusion coefficient for garnet for the Fe-Mg interdiffusion coefficient with $D_0 = 9.81 \times 10^{-9}$ m²/s and $Q = 239$ kJ/mol, noting the excellent agreement between the Mg self-diffusion data used and the Fe-Mg interdiffusion data of Lasaga et al. (1977). Substituting

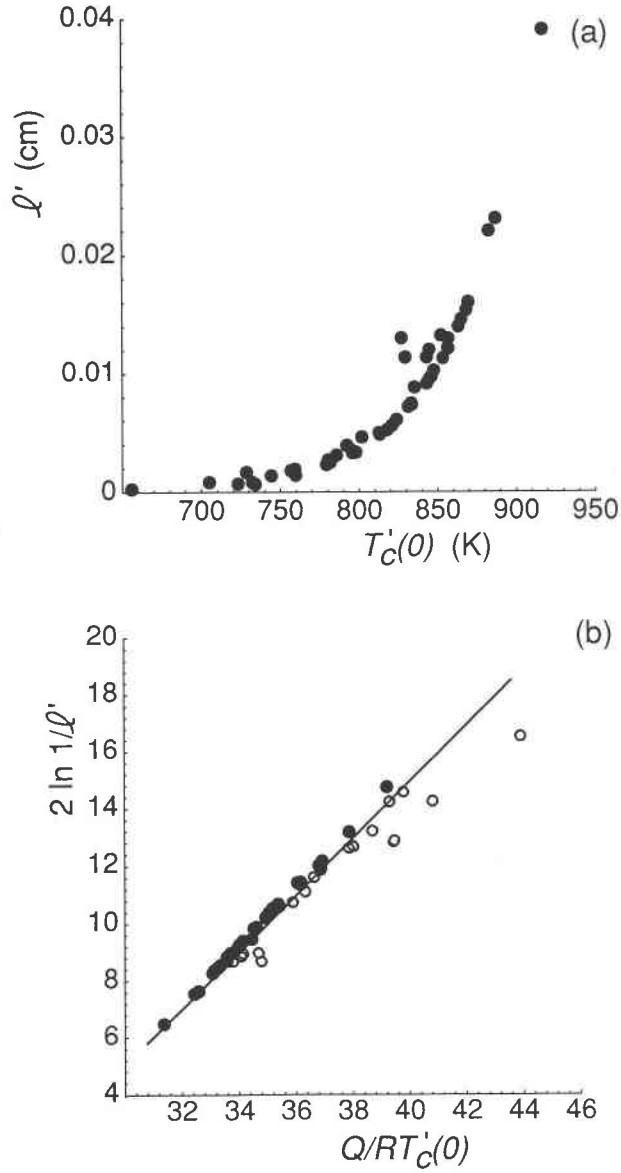

Fig. 6. A Monte Carlo simulation of 50 garnet + biotite pairs, with a prescribed cooling history of $s = 10$ K/m.y. **(a)** Relationship of apparent grain size, l', to apparent closure temperature, $T'_c(0)$. **(b)** A plot of $Q/RT'_c(0)$ vs. 2 ln $1/l'$. The grains that lie above the regression line (solid circles) are the ones that were cut closest to their centers. Open circles are grains cut away from their centers.

these diffusion parameters into Equation 4 and transforming $s(y)$ into units of kelvins per million years give

$$s(y) = 10.7478\left[\frac{T'_c(y)}{l'}\right]^2 (1 - y^2)\exp\left[G(y) - \frac{28784}{T'_c(y)}\right]. \quad (7)$$

The loci on a $T'_c(y)$ − ln $s(y)$ diagram may be calculated iteratively, by means of Equation 5, or generated directly,

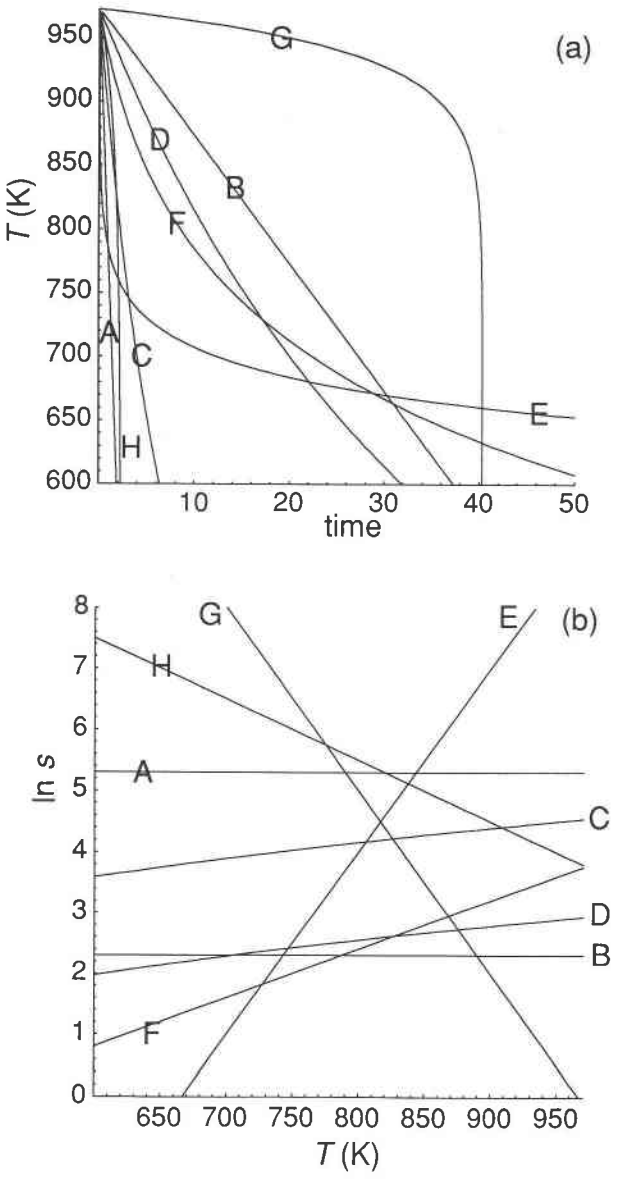

Fig. 7. (a) Four qualitatively different temperature-time histories chosen for the simulations. For each there are two realistic end-member situations, fast and slow. Thermal histories of A and B are linear in T: (A) $t = t_0 + {}^1/_{200}(T - T_0)$; (B) $t = t_0 + {}^1/_{10}(T - T_0)$. C and D are linear in T^{-1}: (C) $t = t_0 + {}^1/_{-0.0001}({}^1/_{T_0} - {}^1/_T)$; (D) $t = t_0 + {}^1/_{-0.00002}({}^1/_{T_0} - {}^1/_T)$. E–H are exponential in T: (E) $t = t_0 + {}^{e^{20}}/_{0.03}(e^{-0.03T_0} - e^{-0.03T})$; (F) $t = t_0 + {}^{e^4}/_{0.008}(e^{-0.008T_0} - e^{-0.008T})$; (G) $t = t_0 + {}^{e^{-29}}/_{-0.03}(e^{0.03T_0} - e^{0.03T})$; (H) $t = t_0 + {}^{e^{-13.5}}/_{-0.01}(e^{0.01T_0} - e^{0.01T})$. T_0 is the peak metamorphic temperature at the starting time, t_0, (b) The corresponding temperature-cooling rate histories are (A) $\ln s = 200$, (B) $\ln s = 10$, (C) $s = -0.0001T^2$, (D) $s = -0.00002T^2$, (E) $\ln s = 0.03T - 20$, (F) $\ln s = 0.008T - 4$, (G) $\ln s = -0.03T + 29$, and (H) $\ln s = -0.01T + 13.5$.

using our observation that the slopes of the loci have the following approximate form (Fig. 5):

$$\frac{d \ln s(y)}{dT'_c(y)} = a + \frac{b}{T'_c(0)^2}.$$

The loci may then be represented by the following equation:

$$\ln s(y) = \ln s(0) + [T'_c(y) - T'_c(0)]\left[a + \frac{b}{T'_c(0)^2}\right]. \quad (8)$$

For the diffusion data used here and for spherical geometry [so $G(0) = 1.964$: Dodson 1986, Table 2], values for a and b are -0.00113 and 11300, respectively. In Equation 8, it is assumed that the cooling rate remains constant during the closure of each grain. If the cooling rate changes quickly during cooling, the actual locus departs progressively from the calculated locus as y increases.

Simulations

To test the efficacy of this approach, a Monte Carlo study was performed to simulate garnet-biotite closure relationships for samples involving many garnet grains with different section positions and for four simplified, but qualitatively different, thermal histories that may characterize different tectonic settings (Fig. 7a). For each thermal history, two T-t histories were chosen that represent geologically fast and slow cooling histories. The corresponding temperature–cooling rate histories (Fig. 7b) were obtained by differentiating the T-t histories.

To generate the data in the simulations, a log-normal distribution of actual grain radii, l, and a uniform distribution of section positions were assumed. From these distributions, l and x were calculated randomly. These data were used to calculate apparent grain radii, l'. The apparent closure temperatures were calculated with Equation 1, using the prescribed cooling histories (Fig. 7b) and the generated l and x values. The apparent cooling rates were calculated with Equation 4, assuming $x = 0$, using the apparent grain radii and closure temperatures. The resulting data involve sets of l', $T'_c(y)$, and $s(y)$ values that correspond to the form of a data set typically obtained from natural samples. Loci were calculated using Equation 8. The l' and $T'_c(y)$ values were used to identify those grains that are most likely to be cut near their centers (Fig. 6b). These grains and their loci were indicated on $T'_c(y)$ – $\ln s(y)$ diagrams to compare them with the prescribed cooling histories.

The results of the simulations for eight cooling histories are shown in Figure 8. Grains that were cut close to their centers always clustered around the prescribed cooling history (Fig. 8). For shallow slopes and steep negative slopes of cooling rate histories, grains aligned on the prescribed cooling history (Fig. 8a–8d, 8f, 8h). For very steep positive slopes, all grains approximated the prescribed cooling history. Thus the method appears to work well in defining a cooling rate history. Simulations suggest that if many garnets are analyzed grains may be identified that define the cooling rate history and that this approach is valid for the wide range of cooling rate histories tested (Fig. 7).

Application to rocks

The results from the simulations are promising and suggest that this may be a straightforward method of dis-

tinguishing among qualitatively different cooling rate histories. An outline of a procedure for estimating the cooling rate histories of rocks follows below. Several complexities associated with the steps in this outline are briefly discussed following the procedure: (1) Select rocks with garnet and biotite as the only Fe-Mg minerals. (2) Find garnets that have retrograde zoning, lack biotite inclusions, and are surrounded by sufficient biotite; neither garnet nor biotite should show evidence of resorption or growth. (3) Analyze the centers of the garnet grains and measure their grain size. (4) Analyze the adjacent biotite and make sure that the biotite is homogeneous in the area surrounding the garnet. (5) Calculate the garnet-biotite Fe-Mg K_D from the mineral analyses. (6) Calculate $T'_c(0)$ using Equation 6 and the K_D values. (7) Calculate $s(0)$, assuming $y = 0$, using Equation 7, the above-calculated $T'_c(0)$, and the measured grain radius. (8) Calculate the loci using Equation 8, the above-calculated $T'_c(0)$ and $s(0)$, and the assumed temperature at the start of cooling; show them on a $T'_c(y)$ vs. ln $s(y)$ plot, as in Figure 8. (9) Identify the best grains, as in Figure 6. (10) Indicate these best grains on the $T'_c(y)$ vs. ln $s(y)$ plot, their trend giving the cooling rate history. (11) Evaluate uncertainties.

In relation to steps 1 and 4, biotite and garnet must not have equilibrated with other Fe-Mg phases during cooling. In relation to step 2, note that larger garnets in thin section may preserve growth zoning, whereas smaller garnets equilibrated at, and following, the metamorphic peak. In relation to steps 2 and 4, sufficient biotite refers to the region of homogeneous biotite composition around the garnet, with a mode 1.5 times that of garnet, if the garnet is completely surrounded by biotite and volume diffusion is the dominant process (see above). If the garnet is surrounded by e.g., a biotite + quartz + feldspar matrix, it is less clear what the minimum mode of biotite should be. If grain boundary diffusion is faster than volume diffusion through biotite, then the minimum mode is smaller than for volume diffusion. However, there is currently insufficient information (cf. Eiler et al., 1992). In relation to steps 5 and 6, if the garnet or biotite contains elements in addition to Fe and Mg, the K_D should be written in terms of these additional elements. In addition, corrections in the geothermometer may need to be included to account for nonideality. However, the effects of additional components on the relationship between the closure temperature and the grain size are not known, and it is difficult to assess the validity of the corrections. It is also possible that the magnitude of corrections on closure temperature due to additional components is small compared with the variation in closure temperature caused by grain size variation. When using Equation 7, it is assumed that the equilibration between garnet and biotite is dominated by Fe-Mg interdiffusion (step 7). Retrograde zoning of Ca or Mn in the garnet might indicate that this is not a good assumption. In relation to step 11 it is important to distinguish between systematic and random uncertainties (e.g., Powell and Holland, 1988). The position of a set of loci might not be well known on a $T'_c(y)$ vs. ln $s(y)$ diagram, but on

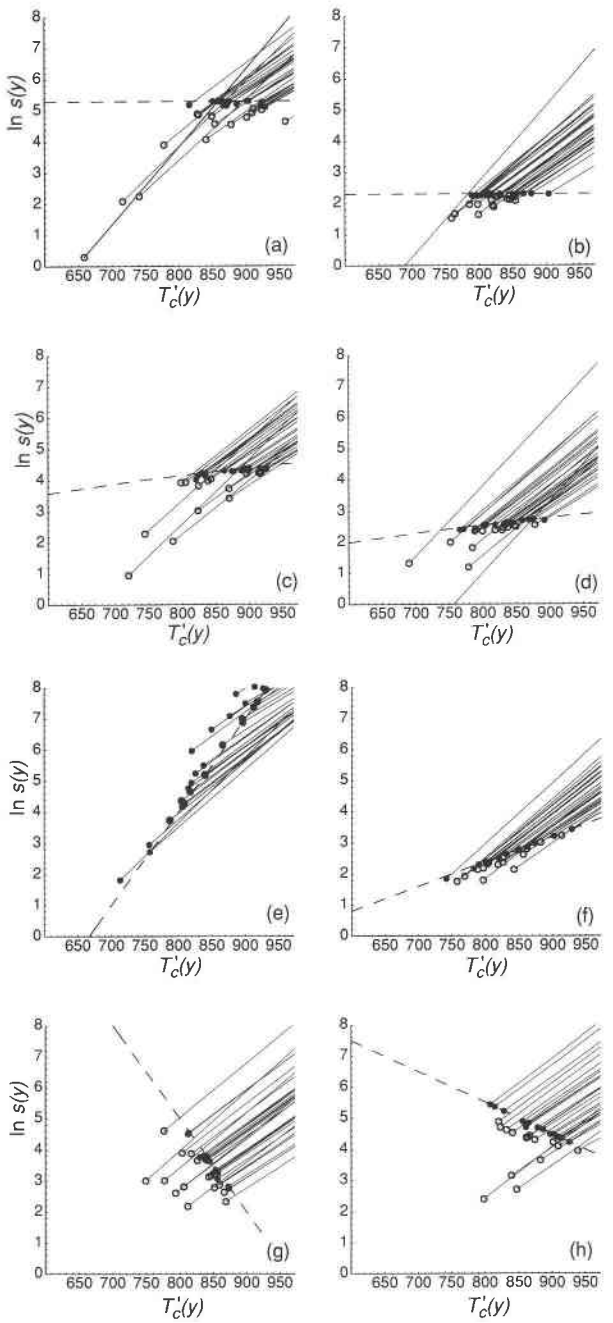

Fig. 8. A Monte Carlo simulation of 30 garnet + biotite pairs, with radius l, random log-normal from $\mu_l = 4.26$ and $\sigma_l = 0.82$, and x random uniform. **(a** and **b)** The prescribed cooling history is linear in s and given by a dashed line; **(c** and **d)** simulations for two thermal histories that are linear in T^{-1}. The prescribed cooling histories (parts **a–d**) correspond to the capital letters in Fig. 7b; solid lines are ln $s(y)$ vs. $T'_c(y)$ loci; solid circles identify grains cut close to their centers; open circles are other grains. Note that solid circles closely correspond to the prescribed cooling rate history. $T'_c(y)$ is in kelvins and $s(y)$ in kelvins per million years. **(e–f)** A Monte Carlo simulation for two exponential cooling histories, with cooling rates increasing with temperature and **(g–h)** with cooling rates that decrease with temperature. In each case, the prescribed cooling history is given by the dashed line, with the peak metamorphic temperature at $T_0 = 973$ K.

varying the parameters involved, the set of loci moves around on the diagram in a highly systematic way. Systematic uncertainties derived from the diffusion parameters of garnet (Q and D_0) and the parameters in the geothermometer equation may shift the set of loci by 2 log units in ln $s(y)$ and 100 K in $T_c'(y)$. However, in general, the form of the implied cooling rate history is hardly affected by these uncertainties. On the other hand, random uncertainties affect the relative positions of the loci. Random uncertainties include those from the measurement of the mineral compositions and the garnet grain size. The uncertainties in $T_c'(0)$ and $s(0)$ contributed by the random uncertainties are likely to be much less than those contributed by the systematic errors, e.g., < 1 log unit in ln $s(0)$ and 30 K in $T_c'(0)$.

The uncertainties in $T_c(x)$ and Q cease to be systematic if several geothermometers and their close relationships are used. Given the current status of diffusion data for minerals and geothermometer equations, combining data from several systems is unlikely to be successful.

Discussion

This method is potentially valuable in the study of orogenic belts. From a T_c-s relationship, the relative T-t relationship can be deduced by integration. For example, the exponential cooling rate history from one of the simulations (Fig. 7, curve H),

$$\frac{dT}{dt} = s = e^{(13.5-0.01T)}$$

may be integrated with respect to t and rearranged to give a time history of

$$t = t_0 + \frac{e^{-13.5}}{-0.01}(e^{0.01T_0} - e^{0.01T})$$

in which T_0 is the temperature at time, t_0, i.e., the start of cooling, which may be the peak metamorphic temperature. If t_0 can be estimated, for example by radiometric dating, and estimates of T_0 from other petrological constraints are available, then the rest of the T-t evolution can be derived from the closure relationships. Natural thermal histories are likely to have a shape related to the error function (Carslaw and Jaeger, 1959). However, such cooling histories can be closely approximated by exponential histories or histories that are linear in T^{-1}. The qualitative shape of the T-t histories may be used to distinguish among tectonic environments. For example, cooling rates resulting from erosion-driven environments increase exponentially with cooling, where cooling rates resulting from advectively heated processes decrease exponentially with cooling.

Acknowledgments

We would like to thank Thomas Chacko, Sumit Chakraborty, Barbara Dutrow, and Darrell Henry for helpful reviews. Financial support for this research was provided by the Australian Research Committee.

References cited

Carslaw, H.S., and Jaeger, J.C. (1959) Conduction of heat in solids (2nd edition), 510 p. Clarendon, Oxford, U.K.

Cygan, R.T., and Lasaga, A.C. (1985) Self-diffusion of magnesium in garnet at 750° to 900 °C. American Journal of Science, 285, 328–350.

Dodson, M.H. (1973) Closure temperature in cooling geochronological and petrological systems. Contributions to Mineralogy and Petrology, 40, 259–274.

——— (1986) Closure profiles in cooling systems. Material Science Forum, 7, 145–154.

Ehlers, K., and Powell, R. (1994) An empirical modification of Dodson's equation for closure temperature in binary systems. Geochimica et Cosmochimica Acta, 58, 241–248.

Eiler, J.M., Baumgartner, L.P., and Valley, J.W. (1992) Intercrystalline stable isotope diffusion: A fast grain boundary model. Contributions to Mineralogy and Petrology, 112, 543–557.

England, P.C., and Thompson, A.B. (1984) Pressure-temperature-time path of regional metamorphism. I. Heat transfer during the evolution of regions of thickened continental crust. Journal of Petrology, 25, 894–928.

Holland, T.J.B., and Powell, R. (1990) An enlarged and updated internally consistent thermodynamic dataset with uncertainties and correlations: The system K_2O-Na_2O-CaO-MgO-MnO-FeO-Fe_2O_3-Al_2O_3-TiO_2-SiO_2-C-H_2-O_2. Journal of Metamorphic Geology, 8, 89–124.

Jenkin, G.R.T., Fallick, A.E., Farrow, C.M., and Bowes, G.E. (1991) COOL: A Fortran-77 computer program for modelling stable isotopes in cooling closed systems. Computer and Geosciences, 17, 391–412.

Lasaga, A.C. (1983) Geospeedometry: An extension of geothermometry. In S.K. Saxena, Ed., Kinetics and equilibrium in mineral reactions, p. 82–114. Springer-Verlag, New York.

Lasaga, A.C., Richardson, S.M., and Holland, H.D. (1977) The mathematics of cation diffusion and exchange between silicate minerals during retrograde metamorphism. In S.K. Saxena and S. Bhattachanji, Eds., Energetics of geological processes, p. 353–388. Springer-Verlag, New York.

Lovera, O.M., Richter, F.M., and Harrison, T.M. (1989) The $^{40}Ar/^{39}Ar$ thermochronometer for slowly cooled samples having a distribution of diffusion domain sizes. Journal of Geophysical Research, 94, 17917–17935.

Lux, D.R., De Yoreo, J.J., Guldotti, C.V., and Decker, E.R. (1986) Role of plutonism on low pressure metamorphic belt formation. Nature, 323, 794–796.

Onorato, P.I.K., Yinnon, H., Uhlmann, D.R., and Taylor, L.A. (1979) Partitioning as a cooling rate indicator. Proceedings of the 10th Lunar Science Conference, 479–491.

Ozawa, K. (1984) Olivine-spinel geospeedometry: Analysis of diffusion-controlled Mg-Fe^{2+} exchange. Geochimica et Cosmochimica Acta, 48, 2597–2611.

Powell, R., and Holland, T.J.B. (1988) An internally-consistent dataset with uncertainties and correlations. III. Applications to geobarometry, worked examples and a computer program. Journal of Metamorphic Geology, 6, 173–204.

Sandiford, M., Martin, N., Zhou, S., and Fraser, G. (1991) Mechanical consequences of granite emplacement during high-T low-P metamorphism and the origin of "anticlockwise" PT paths. Earth and Planetary Science Letters, 107, 164–171.

Spear, F.S., and Peacock, S.M. (1989) Metamorphic pressure-temperature-time paths. American Geophysical Union Short Course in Geology, 7, 102 p.

Thompson, A.B., and England, P.C. (1984) Pressure temperature time path of regional metamorphism. II. Their inference and interpretation using mineral assemblages. Journal of Petrology, 25, 929–955.

Manuscript received May 20, 1993
Manuscript accepted March 8, 1994